THE EUROPEAN
PHYSICAL JOURNAL C

Regular Article - Theoretical Physics

# On the effect of the degeneracy among dark energy parameters

**Yungui Gong**[1,2,a], **Qing Gao**[1,b]

[1] MOE Key Laboratory of Fundamental Quantities Measurement, School of Physics, Huazhong University of Science and Technology, Wuhan 430074, Hubei, China
[2] Institute of Theoretical Physics, Chinese Academy of Sciences, Beijing 100190, China

**Abstract** The dynamics of scalar fields as dark energy is well approximated by some general relations between the equation of state parameter $w(z)$ and the fractional energy density $\Omega_\phi$. Based on the approximation, for slowly rolling scalar fields, we derived the analytical expressions of $w(z)$ which reduce to the popular Chevallier–Polarski–Linder parametrization with an explicit degeneracy relation between $w_0$ and $w_a$. The models approximate the dynamics of scalar fields well and help eliminate the degeneracies among $w_a$, $w_0$, and $\Omega_{m0}$. With the explicit degeneracy relations, we test their effects on the constraints of the cosmological parameters. We find that: (1) The analytical relations between $w_0$ and $w_a$ for the two models are consistent with observational data. (2) The degeneracies have little effect on $\Omega_{m0}$. (3) The $1\sigma$ error of $w_0$ was reduced about 30 % with the degeneracy relations.

## 1 Introduction

To explain the cosmic acceleration found by the observations of type Ia supernovae (SNe Ia) in 1998 [1,2], we usually introduce an exotic energy component with negative pressure to the right hand side of the Einstein equation. This exotic energy component, which contributes about 72 % to the total energy density in the universe, is dubbed dark energy. Although the cosmological constant is the simplest candidate for dark energy and is consistent with current observations, other possibilities are also explored due to the discrepancy of many orders of magnitude between the theoretical estimation and astronomical observations for the cosmological constant. Currently we still have no idea about the nature of dark energy. In particular, the question whether dark energy is just the cosmological constant remains unanswered. For reviews of dark energy, please see Refs. [3–9].

One way of studying the nature of dark energy is through the observational data. There are many model-independent studies on the nature of dark energy using the observational data [10–39]. In particular, one usually parameterizes the energy density $\Omega_\phi(z)$ or the equation of state parameter $w(z)$ of the dark energy. Motivated by the tracking solution [40,41] for a wide class of quintessence [42] potentials in which the equation of state parameter $w(z)$ varies slowly, Efstathiou approximated $w(z)$ with $w(z) = w_0 - \alpha \ln(1 + z)$ in the redshift range $z < 4$ [16]. However, the parametrization most used for approximating the dynamics of a wide class of scalar fields is the Chevallier–Polarski–Linder (CPL) parametrization with $w(a) = w_0 + w_a(1 - a)$ [36,37]. Because of the degeneracies among the parameters $\Omega_{m0}$, $w_0$, and $w_a$ in the model, complementary cosmological observations are needed to break the degeneracies. The measurement on the cosmic microwave background anisotropy, the baryon acoustic oscillation (BAO) measurement and the SNe Ia observations provide complementary data.

On the other hand, a minimally coupled scalar field $\phi$ was often invoked to model the quintessence [42–44], and the phantom [45]. For a scalar field with a nearly flat potential, there exist approximate relations between the equation of state parameter $w = p/\rho$ and the energy density parameter $\Omega_\phi$ [40,41,46–52]. As discussed above, the dynamics of scalar fields can be approximated with the CPL parametrization and the generic $w - \Omega_\phi$ relations, so we expect that the degeneracies among the parameters $w_0$, $w_a$, and $\Omega_{\phi0}$ can be broken. By using the generic $w - \Omega_\phi$ relations, we can break the degeneracy between $w(z)$ and $\Omega_\phi(z)$. Furthermore, $w(z)$ can be approximated by the CPL parametrization with $w_a$ expressed as a function of $w_0$ and $\Omega_{\phi0}$, so the two-parameter parametrization reduces to one-parameter parametrization [53]. The CPL parametrization with analytical relations among the model parameters helps tighten the constraints on the model parameters.

a e-mail: yggong@mail.hust.edu.cn
b e-mail: gaoqing01good@163.com

In this paper, we derive two particular CPL models with $w_a$ proportional to $1 + w_0$, and we study the effects of the degeneracy relations between $w_a$ and $w_0$ by using the following data: the three year Supernova Legacy Survey (SNLS3) sample of 472 SNe Ia data with systematic errors [54]; the BAO measurements from the 6dFGS [55], the distribution of galaxies in the Sloan Digital Sky Survey (SDSS) [56] and the WiggleZ dark energy survey [57]; the seven-year Wilkinson Microwave Anisotropy Probe (WMAP7) data [58]; and the Hubble parameter $H(z)$ data [59,60].

## 2 CPL parametrization with degenerate $w_0$ and $w_a$

For a quintessence field, the equation of state parameter $w(z)$ is related with its fractional energy density $\Omega_\phi = 8\pi G\rho_\phi/3H^2$ as follows [49]:

$$1 + w(z) = \kappa^2(\phi)\Omega_\phi(z)(1 - w(z))^2/6, \tag{1}$$

$$\frac{d\phi}{d\ln a} = -\kappa(\phi)\Omega_\phi(z)(1 - w(z)), \tag{2}$$

where $\kappa(\phi) = -3H\dot\phi/V(\phi)$. For scalar fields satisfying the slow-roll conditions,

$$\left(\frac{1}{V}\frac{dV}{d\phi}\right)^2 \ll 1, \quad \frac{1}{V}\frac{d^2V}{d\phi^2} \ll 1, \tag{3}$$

the dark energy density $\rho_\phi(a)$ is nearly constant and it deviates from the cosmological constant by the order $\int_a^1(1 + w)da/a$. Since $1 + w(z) \ll 1$, to the zeroth order approximation, the fractional energy density $\Omega_\phi(a)$ can be replaced by the cosmological constant

$$\Omega_\Lambda(a) = \left[1 + (\Omega_{\phi 0}^{-1} - 1)a^{-3}\right]^{-1}, \tag{4}$$

and the dynamics of the potential can be approximated by the linear expansion of $\kappa(\phi)$ as $\kappa(\phi) = \kappa_0 + \kappa_1(\phi - \phi_0)$ [49]. With these approximations, $w(a)$ was derived as [49]

$$w(a) = -1 + \frac{2}{3}\kappa_0^2\Omega_\Lambda(a)\left[\frac{\Omega_\Lambda(a)}{a^3\Omega_{\phi 0}}\right]^{2\kappa_1/3}. \tag{5}$$

On the other hand, $w(z) = \gamma - 1$ also satisfies the relation [46]

$$\frac{d\gamma}{d\Omega_\phi} = \frac{-3\gamma(2 - \gamma) + \lambda(2 - \gamma)\sqrt{3\gamma\Omega_\phi}}{3(1 - \gamma)\Omega_\phi(1 - \Omega_\phi)}, \tag{6}$$

where $\lambda(\phi) = -V^{-1}(\phi)dV(\phi)/d\phi$. For slow-roll scalar fields, $\gamma \ll 1$ and $\lambda$ is almost constant. Assuming that $\lambda(\phi) = \lambda(\phi)_{\phi=\phi_0} = \lambda_0$, a general relationship between $w$ and the energy density $\Omega_\phi$ for both quintessence and phantom models was found [46,47,61],

$$1 + w = (1 + w_0)\left[\frac{1}{\sqrt{\Omega_\phi}} - \left(\frac{1}{\Omega_\phi} - 1\right)\tanh^{-1}(\sqrt{\Omega_\phi})\right]^2$$
$$\times\left[\frac{1}{\sqrt{\Omega_{\phi 0}}} - (\Omega_{\phi 0}^{-1} - 1)\tanh^{-1}\sqrt{\Omega_{\phi 0}}\right]^{-2}. \tag{7}$$

Note that the above result holds for thawing models [62] with the potentials satisfying the slow-roll conditions (3). It does depend on the specific form of the potential $V(\phi)$; furthermore, it also approximates the dynamics of tachyon fields [61,63]. When $w$ is close to $-1$, the fractional energy density $\Omega_\phi$ can to the zeroth order be approximated by the cosmological constant $\Omega_\Lambda$ [46,47,49], so

$$w(a) = -1 + (1 + w_0)\left[\frac{1}{\sqrt{\Omega_{\phi 0}}} - (\Omega_{\phi 0}^{-1} - 1)\tanh^{-1}\sqrt{\Omega_{\phi 0}}\right]^{-2}$$
$$\times\left[\sqrt{1 + (\Omega_{\phi 0}^{-1} - 1)a^{-3}} - (\Omega_{\phi 0}^{-1} - 1)a^{-3}\right.$$
$$\left.\times\tanh^{-1}[1 + (\Omega_{\phi 0}^{-1} - 1)a^{-3}]^{-1/2}\right]^2. \tag{8}$$

In accordance with Ref. [46], it is explicitly shown in Fig. 4 that the analytical result (8) fits $w(a)$ well for thawing quintessence models with the potentials $V(\phi) \sim \phi^2$, $V(\phi) \sim \phi^{-2}$, and $V(\phi) \sim \exp(-\lambda\phi)$. In Ref. [47], it was explicitly shown in Fig. 1 that the analytical result (8) gives the behavior of $w(a)$ for thawing phantom models with the potentials $V(\phi) \sim \phi^6$, $V(\phi) \sim \phi^2$, $V(\phi) \sim \phi^{-2}$, and $V(\phi) \sim \exp(-\lambda\phi)$. Therefore, we can use $w(a)$ given by Eq. (8) to approximate the thawing scalar fields. If we Taylor expand $\Omega_\phi(a)$ and $w(a)$ around $a = 1$, we get

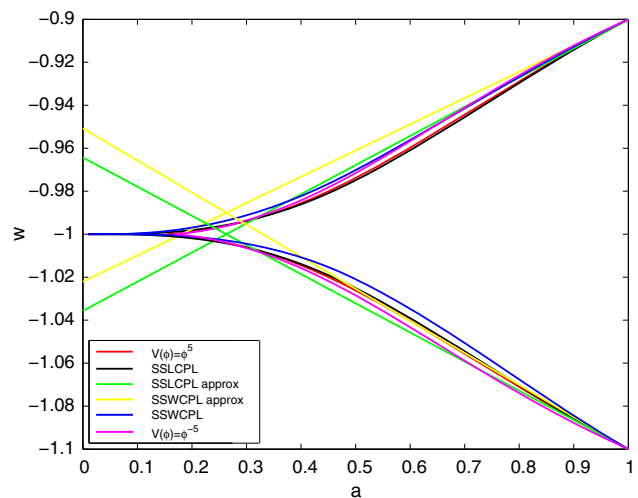$$\Omega_\phi \approx \Omega_{\phi 0}[1 - 3(1 - \Omega_{\phi 0})(1 - a)] \tag{9}$$



**Fig. 1** The evolutions of $w(a)$ for the potentials $V(\phi) \sim \phi^5$ and $V(\phi) \sim \phi^{-5}$, the SSLCPL model (8) and (10) and the SSWCPL model (14) and (16). The initial conditions are taken as $\Omega_{\phi 0} = 0.72$ and $w_0 = -0.9$ for the quintessence and $w_0 = -1.1$ for the phantom

and

$$w = w_0 + 6(1 + w_0)\frac{\Omega_{\phi 0}^{-1/2} - \sqrt{\Omega_{\phi 0}} - (\Omega_{\phi 0}^{-1} - 1)\tanh^{-1}(\sqrt{\Omega_{\phi 0}})}{\Omega_{\phi 0}^{-1/2} - (\Omega_{\phi 0}^{-1} - 1)\tanh^{-1}(\sqrt{\Omega_{\phi 0}})}$$
$$\times (1 - a). \tag{10}$$

Therefore, we derive the CPL parametrization with $w_a$ determined by $w_0$ and $\Omega_{\phi 0}$ starting from Eq. (7). We call this model the SSLCPL model. In particular, we get [53,63]

$$w_a = 6(1 + w_0)\frac{(\Omega_{\phi 0}^{-1} - 1)[\sqrt{\Omega_{\phi 0}} - \tanh^{-1}(\sqrt{\Omega_{\phi 0}})]}{\Omega_{\phi 0}^{-1/2} - (\Omega_{\phi 0}^{-1} - 1)\tanh^{-1}(\sqrt{\Omega_{\phi 0}})}. \tag{11}$$

When $\Omega_{\phi 0} = 0.7$, we get $w_a = -1.42(1 + w_0)$, which is consistent with the numerical result $w \approx w_0 - 1.5(1 + w_0)(1 - a)$ obtained in [46,47]. Note that we derived the analytical expression of $w_a$ within the CPL parametrization which captures the main dynamics of the thawing scalar fields, and this expression is not just a phenomenological dark energy parametrization: it actually approximates the dynamics of thawing scalar fields. For the SSLCPL model, we only have two model parameters $\Omega_{m0}$ and $w_0$ for the spatially flat case. To see how well the approximation performs, in Fig. 1 we show the evolutions of $w(a)$ for the power-law potentials $V(\phi) \sim \phi^5$ and $V(\phi) \sim \phi^{-5}$, and the approximations (8) and (10). It is clear that the relative error brought about by the approximation is under a few percent. For the power-law potential $V(\phi) \sim \phi^n$ with other numbers of power $n$, the relative error is also a few percent.

From the evolution equation satisfied by $\Omega_\phi$,

$$\Omega_\phi' = -3w\Omega_\phi(1 - \Omega_\phi), \tag{12}$$

we take the approximate solution for $\Omega_\phi$ with constant equation of state, $w = w_0$,

$$\Omega_w = \frac{\Omega_{\phi 0}a^{-3w}}{1 - \Omega_{\phi 0} + \Omega_{\phi 0}a^{-3w}}, \tag{13}$$

so

$$w(a) = -1 + (1 + w_0)\left[\frac{1}{\sqrt{\Omega_{\phi 0}}} - (\Omega_{\phi 0}^{-1} - 1)\tanh^{-1}\sqrt{\Omega_{\phi 0}}\right]^{-2}$$
$$\times \left[\sqrt{1 + (\Omega_{\phi 0}^{-1} - 1)a^{3w}} - (\Omega_{\phi 0}^{-1} - 1)a^{3w}\right.$$
$$\left.\times \tanh^{-1}[1 + (\Omega_{\phi 0}^{-1} - 1)a^{3w}]^{-1/2}\right]^2. \tag{14}$$

Then Taylor expansion $\Omega_\phi(a)$ around $a = 1$ gives

$$\Omega_\phi = \{1 + (\Omega_{\phi 0}^{-1} - 1)[1 - 3w(1 - a)]\}^{-1}. \tag{15}$$

Substituting Eq. (15) into Eq. (7), we obtain

$$w(a) = w_0 - 6w_0(1 + w_0)$$
$$\times \frac{(\Omega_{\phi 0}^{-1} - 1)[\sqrt{\Omega_{\phi 0}} - \tanh^{-1}(\sqrt{\Omega_{\phi 0}})](1 - a)}{\Omega_{\phi 0}^{-1/2} - (\Omega_{\phi 0}^{-1} - 1)\tanh^{-1}(\sqrt{\Omega_{\phi 0}})}, \tag{16}$$

so again we get the CPL parametrization with

$$w_a = -6w_0(1 + w_0)\frac{(\Omega_{\phi 0}^{-1} - 1)[\sqrt{\Omega_{\phi 0}} - \tanh^{-1}(\sqrt{\Omega_{\phi 0}})]}{\Omega_{\phi 0}^{-1/2} - (\Omega_{\phi 0}^{-1} - 1)\tanh^{-1}(\sqrt{\Omega_{\phi 0}})}. \tag{17}$$

We call this model the SSWCPL model. For the SSWCPL model, we only have two model parameters, $\Omega_{m0}$ and $w_0$, for the spatially flat case. In Fig. 1, we show the evolutions of $w(a)$ for the approximation (14) and (16). It is clear that the relative errors brought about by the approximations are under a few percent. Contrary to the intuition that the approximation with $\Omega_w$ may be inappropriate, the numerical results show that the relative error due to the approximation is still small, so it is a good approximation. For both the SSLCPL and the SSWCPL models, we find that $w_a \propto 1 + w_0$, so the models are automatically consistent with $\Lambda$CDM model with $w_0 = -1$ and $w_a = 0$. We would like to emphasize that the models we proposed well approximate the dynamics of a wide class of thawing scalar fields in the whole redshift region as shown in Fig. 1; they are different from both $\Lambda$CDM and $w$CDM models which cannot the approximate dynamical scalar fields, and they eliminate the degeneracy between $w_0$ and $w_a$ for the CPL parametrization. Although the CPL parametrization remains a good approximation for the dynamics of a wide class of scalar fields at low redshifts, the degeneracy among the model parameters is still a problem for the fitting of cosmological data; our models break the degeneracy and help tighten the constraints on cosmological models.

## 3 Observational constraints

We apply the SNe Ia, BAO, WMAP7, and the Hubble parameter $H(z)$ data to test the effects of the degeneracy relations (11) and (17) on the constraints of $\Omega_{m0}$ and $w_0$. The SNLS3 SNe Ia data consist of 123 low-redshift SNe Ia data with $z < 0.1$ mainly from Calan/Tololo, CfAI, CfAII, CfAIII, and CSP, 242 SNe Ia data over the redshift range $0.08 < z < 1.06$ observed from the SNLS [54], 93 intermediate-redshift SNe Ia data with $0.06 < z < 0.4$ observed during the first season of the SDSS-II supernova survey [64], and 14 high-redshift SNe Ia data with $z > 0.8$ from Hubble Space Telescope [65]. For the fitting to the SNLS3 data, we need to add two more nuisance parameters $\alpha$ and $\beta$.

**Fig. 2** The marginalized $1\sigma$ and $2\sigma$ constraints on the flat SSLCPL model. The *upper panels* are for the $1\sigma$ and $2\sigma$ contour plots of $\Omega_{m0} - w_0$ and $w_0 - w_a$. The *lower panels* show the reconstructions of $w(z)$ and $Om(z)$ by using the constraints on $\Omega_{m0}$ and $w_0$
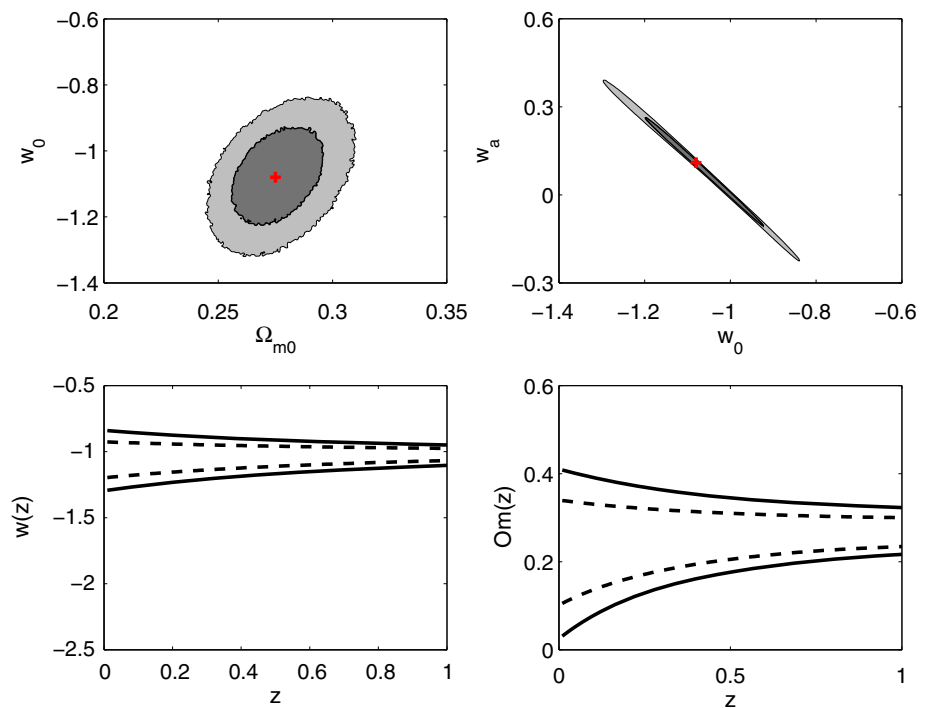


The BAO data [57] consist of the measurement at the redshift $z = 0.106$ from the 6dFGS [55], the measurements of the distribution of galaxies at two redshifts $z = 0.2$ and $z = 0.35$ [56] in the SDSS and the measurements of the acoustic parameter at three redshifts, $z = 0.44$, $z = 0.6$ and $z = 0.73$, from the WiggleZ dark energy survey [57]. For the BAO data, we need to add two more nuisance parameters, $\Omega_b h^2$ and $\Omega_m h^2$.

For the WMAP7 data, we use the measurements of the shift parameter and the acoustic index at the recombination redshift [58], and we need to add two more nuisance parameters $\Omega_b h^2$ and $\Omega_m h^2$.

The Hubble parameter $H(z)$ data consist of the measurements of $H(z)$ at 11 different redshifts obtained from the differential ages of passively evolving galaxies [60,66], and three data points at redshifts $z = 0.24$, $z = 0.34$ and $z = 0.43$, determined by taking the BAO scale as a standard ruler in the radial direction [59]. The $H(z)$ data span to the redshift regions $z = 1.75$.

After obtaining the constraints on the model parameters, we reconstruct $w(z)$ and apply the $Om$ diagnostic [67] to detect the deviation from the $\Lambda$CDM model. $Om(z)$ is defined as

$$Om(z) = \frac{E^2(z) - 1}{(1+z)^3 - 1}, \qquad (18)$$

where the dimensionless Hubble parameter $E(z) = H(z)/H(z=0)$.

Now we consider the effects of the degeneracy relations (11) and (17) on $\Omega_{m0}$ and $w_0$ for the spatially flat case $\Omega_{k0} =$ 0. Fitting the SSLCPL model to the observational data, we get the marginalized $1\sigma$ constraints $\Omega_{m0} = 0.275^{+0.015}_{-0.011}$ and $w_0 = -1.08^{+0.11}_{-0.09}$ with $\chi^2 = 432.6$. By using the degeneracy relation (11) and the correlation between $\Omega_{m0}$ and $w_0$, we derived the marginalized $1\sigma$ constraint $w_a = 0.11^{+0.12}_{-0.14}$. We show the marginalized $1\sigma$ and $2\sigma$ contours of $\Omega_{m0}$ and $w_0$, and $w_0$ and $w_a$ in Fig. 2. By using the correlation between $\Omega_{m0}$ and $w_0$, we reconstruct the evolutions of $w(z)$ and $Om(z)$ in Fig. 2.

Fitting the SSWCPL model to the observational data, we get the marginalized $1\sigma$ constraints $\Omega_{m0} = 0.276^{+0.014}_{-0.013}$ and $w_0 = -1.09 \pm 0.10$ with $\chi^2 = 432.6$. By using the degeneracy relation (17) and the correlation between $\Omega_{m0}$ and $w_0$, we derived the marginalized $1\sigma$ constraint $w_a = 0.12^{+0.16}_{-0.15}$. We show the marginalized $1\sigma$ and $2\sigma$ contours of $\Omega_{m0}$ and $w_0$, and $w_0$ and $w_a$ in Fig. 3. By using the correlation between $\Omega_{m0}$ and $w_0$, we reconstruct the evolutions of $w(z)$ and $Om(z)$ in Fig. 3.

Fitting the CPL model to the observational data, we get the marginalized $1\sigma$ constraints $\Omega_{m0} = 0.278^{+0.018}_{-0.011}$, $w_0 = -1.0^{+0.17}_{-0.13}$ and $w_a = -0.33^{+0.53}_{-1.03}$ with $\chi^2 = 432.4$. We show the marginalized $1\sigma$ and $2\sigma$ contours of $\Omega_{m0}$ and $w_0$, and $w_0$ and $w_a$ in Fig. 4. By using the correlations among the parameters, we reconstruct the evolutions of $w(z)$ and $Om(z)$ in Fig. 4. These results are summarized in Table 1.

Before comparing the constraints for the SSLCPL and SSWCPL models with the familiar CPL model, we need to check the consistencies of the degeneracy relations (11) and (17). So we put the $2\sigma$ contour plots of $w_0$ and $w_a$ from Figs. 2, 3 and 4 together in Fig. 5. We see that the analytical

**Fig. 3** The marginalized $1\sigma$ and $2\sigma$ constraints on the flat SSWCPL model. The *upper panels* are for the $1\sigma$ and $2\sigma$ contour plots of $\Omega_{m0} - w_0$ and $w_0 - w_a$. The *lower panels* show the reconstructions of $w(z)$ and $Om(z)$ by using the constraints on $\Omega_{m0}$ and $w_0$
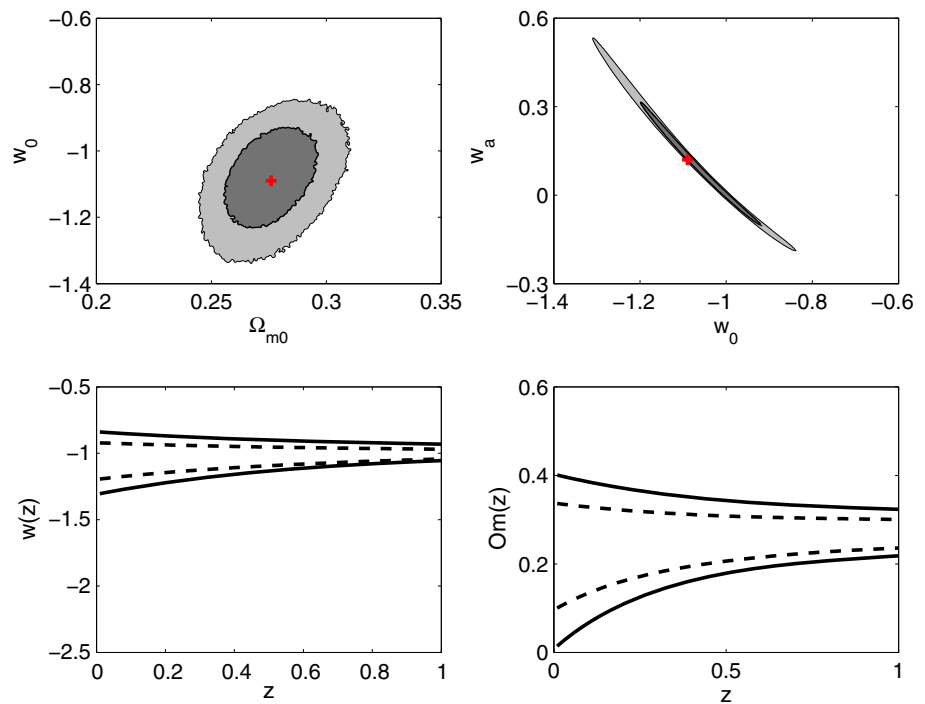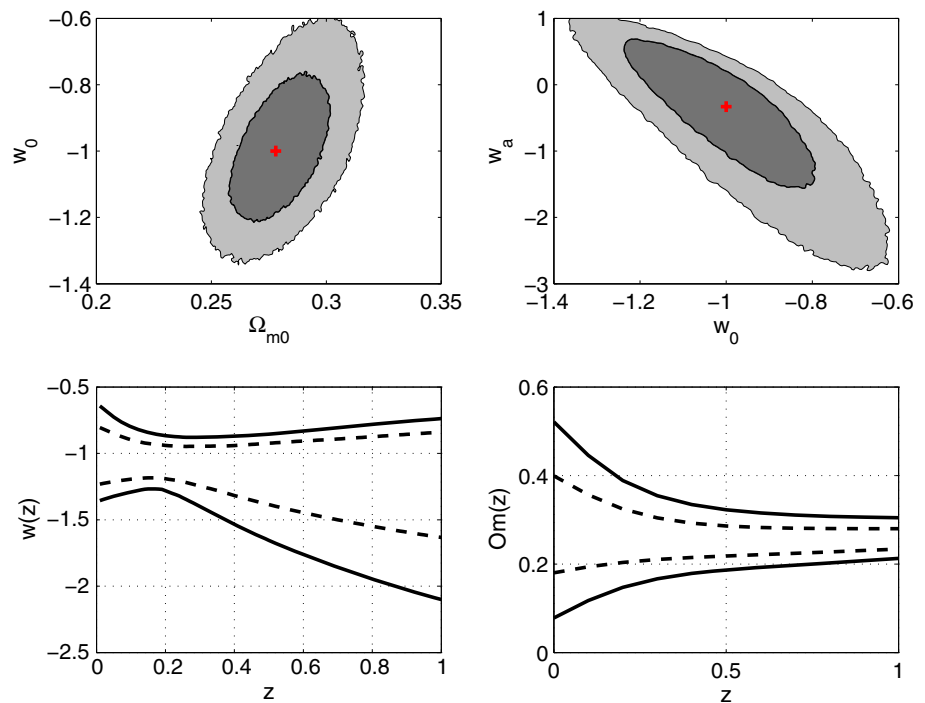


**Fig. 4** The marginalized $1\sigma$ and $2\sigma$ constraints on the flat CPL model. The *upper panels* are for the $1\sigma$ and $2\sigma$ contour plots of $\Omega_{m0} - w_0$ and $w_0 - w_a$. The *lower panels* are the reconstructions of $w(z)$ and $Om(z)$ by using the constraints on $\Omega_{m0}$, $w_0$, and $w_a$



**Table 1** The marginalized $1\sigma$ constraints from observational data

| Model | $\Omega_m$ | $w_0$ | $w_a$ |
|---|---|---|---|
| Flat SSLCPL | $0.275^{+0.015}_{-0.011}$ | $-1.08^{+0.11}_{-0.09}$ | $0.11^{+0.12}_{-0.14}$ |
| Flat SSWCPL | $0.276^{+0.014}_{-0.013}$ | $-1.09 \pm 0.10$ | $0.12^{+0.16}_{-0.15}$ |
| Flat CPL | $0.278^{+0.018}_{-0.011}$ | $-1.0^{+0.17}_{-0.13}$ | $-0.33^{+0.53}_{-1.03}$ |

degeneracies (11) for the SSLCPL model and (17) for the SSWCPL model are consistent with the $w_0 - w_a$ contour for the CPL model obtained from the observational constraints, and the variation of $w(z)$ $(w_a)$ is constrained much tighter with the help of analytical relations (11) and (17). The effects of the degeneracy relations (11) and (17) on $\Omega_{m0}$ are minimal. The $1\sigma$ errors of $w_0$ for SSLCPL and SSWCPL models

**Fig. 5** The marginalized $2\sigma$ contours of $w_0$ and $w_a$ for the SSLCPL, SSWCPL and CPL models
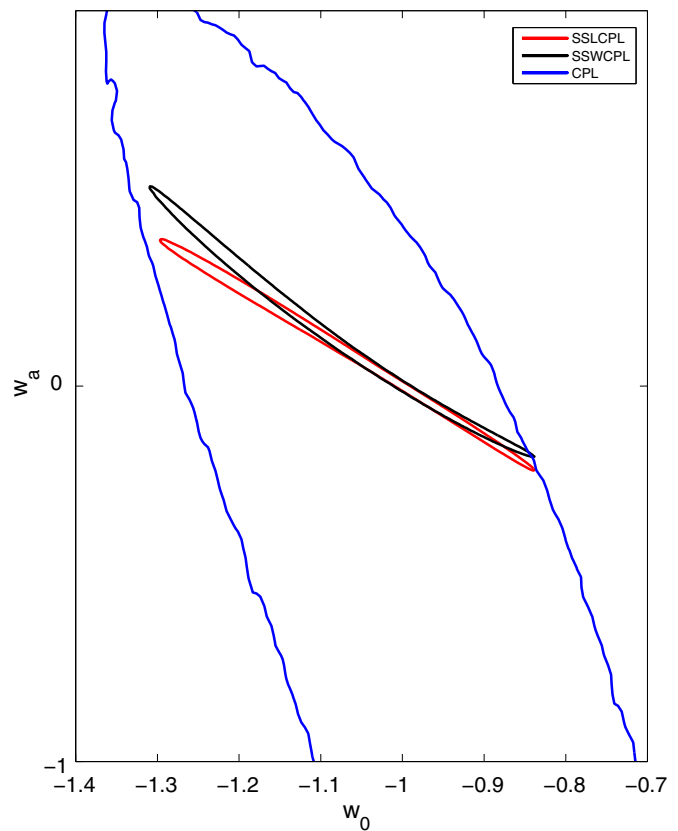


are reduced around 30 % with the degeneracy relations (11) and (17) compared with that in CPL model. Comparing the results from the three models, we find that all three models fit the observational data well because they give almost the same value of $\chi^2$. In terms of the Akaike information criterion (AIC) [68] or Bayesian information criterion (BIC) [69], the SSLCPL and SSWCPL models fit the observational data a little better than the CPL model does. All three models are consistent with $\Lambda$CDM model at the $1\sigma$ level, as shown explicitly by the $w(z)$ and $Om(z)$ plots in Figs. 2, 3 and 4.

With the constraints on the model parameters $\Omega_{m0}$ and $w_0$, we get the constraints on the forms of the thawing potential $V(\phi)$ by using the following relations:

$$\left(\frac{d\phi}{d\ln a}\right)^2 = 3m_{pl}^2\Omega_\phi(a)|1 + w(a)|, \tag{19}$$

$$V(a) = \frac{1}{2}\rho_{cr0}(1 - w(a))\Omega_\phi(a)(H(a)/H_0)^2, \tag{20}$$

where $m_{pl} = (8\pi G)^{-1/2}$ and the current critical density $\rho_{cr0} = 3m_{pl}^2 H_0^2$. The allowed $1\sigma$ regions of the thawing potentials for the phantom and quintessence cases are shown in Fig. 6. For the phantom case, the scalar field climbs up the potential, the potential $V(\phi) = \phi^{0.85}$ shown with the dashed line is inside the allowed $1\sigma$ region. For the quintessence case, the scalar field rolls down the potential, the potential
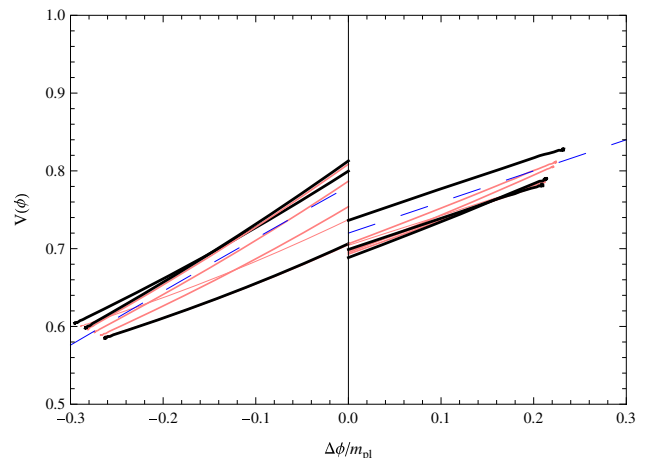


**Fig. 6** The $1\sigma$ constraint on the thawing potential. The *left side* is for the phantom field and the *right side* is for the quintessence field. The potential is in units of the current critical density $\rho_{cr0}$. $\Delta\phi$ is the difference between the scalar field $\phi$ and its current value $\phi_0$. The *dashed lines* show the potential $V(\phi) = \phi^{0.85}$ for the phantom case and $V(\phi) = \phi$ for the quintessence case

$V(\phi) = \phi$ shown with the dashed line is inside the allowed $1\sigma$ region.

## 4 Conclusions

From the relationship (7) for thawing models with a nearly flat potential and the CPL approximation for a wide class

of dynamical dark energy models, we derived the SSLCPL and SSWCPL models which break the degeneracies among $\Omega_{\phi 0}$, $w_0$ and $w_a$. The two models reduce to the CPL model with only one free parameter $w_0$. The relative errors on the equation of state due to the SSLCPL and SSWCPL approximations are under a few percent, so these models capture the main dynamics of the thawing model and approximate the dynamics of a wide class of thawing models well. Instead of studying a particular dynamical dark energy model, the SSLCPL and SSWCPL models can be used to probe the general properties of dynamical dark energy. The proposed degeneracy relations for $w_0$ and $w_a$ are consistent with that found for the familiar CPL model, so the SSLCPL and SSWCPL models are self-consistent. Current observational data constrain the current value of the equation of state $w_0$ of dark energy around $-1$ with more than 10 % error. The current value of the variation of the equation of state $w_a$ is loosely constrained, with the relation between $w_0$ and $w_a$ which is proportional to $1 + w_0$ found in the SSLCPL and SSWCPL models; $w_a$ is tightly constrained and $w_0 \leq -1$ at the $1\sigma$ level. Both models give almost the same minimum $\chi^2$ as the original CPL does when fitting to the observational data. In terms of AIC or BIC, the models fit the observational data a little better than the original CPL does. With the help of the relations (11) and (17), the $1\sigma$ error bar of $w_0$ is reduced by about 30 %. The result is almost the same when we replace the WMAP7 data by the Planck data [70–72]. Both the SSLCPL and the SSWCPL models have only one free parameter and they help tighten the constraint on the property of dark energy.

With the tighter constraints on the parameters $\Omega_{m0}$ and $w_0$, we obtain the constraints on the thawing potential $V(\phi)$. For the phantom case, the potential $V(\phi) = \phi^{0.85}$ is consistent with current observations. For the quintessence case, the potential $V(\phi) = \phi$ is consistent with current observations.

# References

1. A.G. Riess et al., Astron. J. **116**, 1009 (1998). doi:10.1086/300499
2. S. Perlmutter et al., Astrophys. J. **517**, 565 (1999). doi:10.1086/307221
3. V. Sahni, A.A. Starobinsky, Int. J. Mod. Phys. D **9**, 373 (2000)
4. P. Peebles, B. Ratra, Rev. Mod. Phys. **75**, 559 (2003). doi:10.1103/RevModPhys.75.559
5. T. Padmanabhan, Phys. Rept. **380**, 235 (2003). doi:10.1016/S0370-1573(03)00120-0
6. E.J. Copeland, M. Sami, S. Tsujikawa, Int. J. Mod. Phys. D. **15**, 1753 (2006). doi:10.1142/S021827180600942X
7. R.R. Caldwell, M. Kamionkowski, Ann. Rev. Nucl. Part. Sci. **59**, 397 (2009). doi:10.1146/annurev-nucl-010709-151330
8. M. Bartelmann, Rev. Mod. Phys. **82**, 331 (2010). doi:10.1103/RevModPhys.82.331
9. M. Li, X.D. Li, S. Wang, Y. Wang, Commun. Theor. Phys. **56**, 525 (2011). doi:10.1088/0253-6102/56/3/24
10. U. Alam, V. Sahni, T.D. Saini, A. Starobinsky, Mon. Not. Roy. Astron. Soc. **354**, 275 (2004). doi:10.1111/j.1365-2966.2004.08189.x
11. U. Alam, V. Sahni, A. Starobinsky, JCAP **0406**, 008 (2004). doi:10.1088/1475-7516/2004/06/008
12. V. Barger, Y. Gao, D. Marfatia, Phys. Lett. B **648**, 127 (2007). doi:10.1016/j.physletb.2007.03.021
13. C. Clarkson, M. Cortes, B.A. Bassett, JCAP **0708**, 011 (2007). doi:10.1088/1475-7516/2007/08/011
14. P.S. Corasaniti, E. Copeland, Phys. Rev. D **67**, 063521 (2003). doi:10.1103/PhysRevD.67.063521
15. P. Astier, Phys. Lett. B **500**, 8 (2001). doi:10.1016/S0370-2693(01)00072-7
16. G. Efstathiou, Mon. Not. Roy. Astron. Soc. **310**, 842 (1999). doi:10.1046/j.1365-8711.1999.02997.x
17. B.F. Gerke, G. Efstathiou, Mon. Not. Roy. Astron. Soc. **335**, 33 (2002). doi:10.1046/j.1365-8711.2002.05612.x
18. S. Sullivan, A. Cooray, D.E. Holz, JCAP **0709**, 004 (2007). doi:10.1088/1475-7516/2007/09/004
19. Y. Wang, P. Mukherjee, Astrophys. J. **606**, 654 (2004). doi:10.1086/383196
20. J. Weller, A. Albrecht, Phys. Rev. Lett. **86**, 1939 (2001). doi:10.1103/PhysRevLett.86.1939
21. Q.G. Huang, M. Li, X.D. Li, S. Wang, Phys. Rev. D. **80**, 083515 (2009). doi:10.1103/PhysRevD.80.083515
22. A. Shafieloo, V. Sahni, A.A. Starobinsky, Phys. Rev. D. **80**, 101301 (2009). doi:10.1103/PhysRevD.80.101301
23. R.G. Cai, Int. J. Mod. Phys. D **20**, 1313 (2011). doi:10.1142/S0218271811019499
24. H. Lampeitl, R. Nichol, H. Seo, T. Giannantonio, C. Shapiro et al., Mon. Not. Roy. Astron. Soc. **401**, 2331 (2009). doi:10.1111/j.1365-2966.2009.15851.x
25. P. Serra, A. Cooray, D.E. Holz, A. Melchiorri, S. Pandolfi et al., Phys. Rev. D. **80**, 121302 (2009). doi:10.1103/PhysRevD.80.121302
26. Y. Gong, R.G. Cai, Y. Chen, Z.H. Zhu, JCAP **1001**, 019 (2010). doi:10.1088/1475-7516/2010/01/019
27. Y. Gong, B. Wang, R.G. Cai, JCAP **1004**, 019 (2010). doi:10.1088/1475-7516/2010/04/019
28. N. Pan, Y. Gong, Y. Chen, Z.H. Zhu, Class. Quant. Grav. **27**, 155015 (2010). doi:10.1088/0264-9381/27/15/155015
29. Y. Gong, X.M. Zhu, Z.H. Zhu, Mon. Not. Roy. Astron. Soc. **415**, 1943 (2011). doi:10.1111/j.1365-2966.2011.18846.x
30. Y. Gong, Q. Gao, Z.H. Zhu, Int. J. Mod. Phys. Conf. Ser. **10**, 85 (2012). doi:10.1142/S201019451200579X
31. Y. Gong, Q. Gao, Z.H. Zhu, Mon. Not. Roy. Astron. Soc. **430**, 3142 (2013). doi:10.1093/mnras/stt120
32. X.D. Li, S. Li, S. Wang, W.S. Zhang, Q.G. Huang et al., JCAP **1107**, 011 (2011). doi:10.1088/1475-7516/2011/07/011
33. Z. Li, P. Wu, H. Yu, Phys. Lett. B **695**, 1 (2011). doi:10.1016/j.physletb.2010.10.044
34. Q. Su, Z.L. Tuo, R.G. Cai, Phys. Rev. D **84**, 103519 (2011). doi:10.1103/PhysRevD.84.103519
35. C. Wetterich, Phys. Lett. B **594**, 17 (2004). doi:10.1016/j.physletb.2004.05.008

36. M. Chevallier, D. Polarski, Int. J. Mod. Phys. D **10**, 213 (2001). doi:10.1142/S0218271801000822
37. E.V. Linder, Phys. Rev. Lett. **90**, 091301 (2003). doi:10.1103/PhysRevLett.90.091301
38. H. Jassal, J. Bagla, T. Padmanabhan, Mon. Not. Roy. Astron. Soc. **356**, L11 (2005)
39. E. Barboza, J. Alcaniz, Z.H. Zhu, R. Silva, Phys. Rev. D **80**, 043521 (2009). doi:10.1103/PhysRevD.80.043521
40. I. Zlatev, L.M. Wang, P.J. Steinhardt, Phys. Rev. Lett. **82**, 896 (1999). doi:10.1103/PhysRevLett.82.896
41. P.J. Steinhardt, L.M. Wang, I. Zlatev, Phys. Rev. D **59**, 123504 (1999). doi:10.1103/PhysRevD.59.123504
42. R. Caldwell, R. Dave, P.J. Steinhardt, Phys. Rev. Lett. **80**, 1582 (1998). doi:10.1103/PhysRevLett.80.1582
43. C. Wetterich, Nucl. Phys. B **302**, 668 (1988). doi:10.1016/0550-3213(88)90193-9
44. B. Ratra, P. Peebles, Phys. Rev. D **37**, 3406 (1988). doi:10.1103/PhysRevD.37.3406
45. R. Caldwell, Phys. Lett. B **545**, 23 (2002). doi:10.1016/S0370-2693(02)02589-3
46. R.J. Scherrer, A. Sen, Phys. Rev. D **77**, 083515 (2008). doi:10.1103/PhysRevD.77.083515
47. R.J. Scherrer, A. Sen, Phys. Rev. D **78**, 067303 (2008). doi:10.1103/PhysRevD.78.067303
48. S. Dutta, R.J. Scherrer, Phys. Lett. B **704**, 265 (2011). doi:10.1016/j.physletb.2011.09.034
49. R. Crittenden, E. Majerotto, F. Piazza, Phys. Rev. Lett. **98**, 251301 (2007). doi:10.1103/PhysRevLett.98.251301
50. S. Dutta, R.J. Scherrer, Phys. Rev. D **78**, 123525 (2008). doi:10.1103/PhysRevD.78.123525
51. G. Gupta, E.N. Saridakis, A.A. Sen, Phys. Rev. **D79**, 123013 (2009). doi:10.1103/PhysRevD.79.123013
52. T. Chiba, S. Dutta, R.J. Scherrer, Phys. Rev. D **80**, 043517 (2009). doi:10.1103/PhysRevD.80.043517
53. Q. Gao, Y. Gong, Int. J. Mod. Phys. D **22**, 1350035 (2013). doi:10.1142/S0218271813500351
54. A. Conley, J. Guy, M. Sullivan, N. Regnault, P. Astier et al., Astrophys. J. Suppl. **192**, 1 (2011). doi:10.1088/0067-0049/192/1/1
55. F. Beutler, C. Blake, M. Colless, D.H. Jones, L. Staveley-Smith et al., Mon. Not. Roy. Astron. Soc. **416**, 3017 (2011). doi:10.1111/j.1365-2966.2011.19250.x
56. W.J. Percival et al., Mon. Not. Roy. Astron. Soc. **401**, 2148 (2010). doi:10.1111/j.1365-2966.2009.15812.x
57. C. Blake, E. Kazin, F. Beutler, T. Davis, D. Parkinson et al., Mon. Not. Roy. Astron. Soc. **418**, 1707 (2011). doi:10.1111/j.1365-2966.2011.19592.x
58. E. Komatsu et al., Astrophys. J. Suppl. **192**, 18 (2011). doi:10.1088/0067-0049/192/2/18
59. E. Gaztanaga, A. Cabre, L. Hui, Mon. Not. Roy. Astron. Soc. **399**, 1663 (2009). doi:10.1111/j.1365-2966.2009.15405.x
60. J. Simon, L. Verde, R. Jimenez, Phys. Rev. D **71**, 123001 (2005). doi:10.1103/PhysRevD.71.123001
61. A. Ali, M. Sami, A. Sen, Phys. Rev. D **79**, 123501 (2009). doi:10.1103/PhysRevD.79.123501
62. R. Caldwell, E.V. Linder, Phys. Rev. Lett. **95**, 141301 (2005). doi:10.1103/PhysRevLett.95.141301
63. X. Chen, Y. Gong, The limit on $w'$ for tachyon dark energy (2013). arXiv:1309.2044
64. R. Kessler, A. Becker, D. Cinabro, J. Vanderplas, J.A. Frieman et al., Astrophys. J. Suppl. **185**, 32 (2009). doi:10.1088/0067-0049/185/1/32
65. A.G. Riess, L.G. Strolger, S. Casertano, H.C. Ferguson, B. Mobasher et al., Astrophys. J. **659**, 98 (2007). doi:10.1086/510378
66. D. Stern, R. Jimenez, L. Verde, M. Kamionkowski, S.A. Stanford, JCAP **1002**, 008 (2010). doi:10.1088/1475-7516/2010/02/008
67. V. Sahni, A. Shafieloo, A.A. Starobinsky, Phys. Rev. D **78**, 103502 (2008). doi:10.1103/PhysRevD.78.103502
68. H. Akaike, IEEE Trans. Autom. Control **19**, 716 (1974)
69. G. Schwarz, Ann. Stat. **6**(2), 461 (1978)
70. P. Ade et al., Planck 2013 results. I. Overview of products and scientific results (2013). arXiv:1303.5062
71. Y. Wang, S. Wang, Phys. Rev. D **88**, 043522 (2013). doi:10.1103/PhysRevD.88.043522
72. Q. Gao, Y. Gong, The tension on the cosmological parameters from different observational data (2013). arXiv:1308.5627